Evaluation Analysis of Seasonal GPV Meteorological Data with SSR Mode S Surveillance Data

Sadanari Shigetomi, Tomoyuki Kozuka,
Hironori Totoki and Yoshikazu Miyazawa
Department of Aeronautics and Astronautics
Graduate School of Engineering, Kyushu University
Fukuoka, Japan
s.shigetomi@aero.kyushu-u.ac.jp

Mark Brown, Tadashi Koga and Yutaka Fukuda

Electronic Navigation Research Institute (ENRI)
Tokyo, Japan

Abstract—**SSR (Secondary Surveillance Radar) is used in air traffic control to identify aircraft and determine their positions. SSR Mode S with EHS (Enhanced Surveillance) capability also downlinks DAPs (Downlink Aircraft Parameters) which are intended to enable more accurate ground-based surveillance and trajectory estimation than conventional SSR Mode A/C. However, DAPs has not been positively adopted by current air traffic management systems in Japan because of the limited number of equipped aircraft. In this paper, static air temperature and wind speed are calculated from DAPs data and statistically compared with NWP (Numerical Weather Prediction) GPV (Grid Point Value) data released by the JMA (Japan Meteorological Agency) using RMSE (Root Mean Squared Error). The results show that RMSE increases with the prediction time of the NWP GPV data. The estimation error due to the minimum resolution of DAPs parameters and the effects of aircraft turning maneuvers upon static air temperature and wind speed are also analyzed. The estimation errors due to DAPs resolution are approximately 1.0[K] in static temperature and 0.35 [m/s] in wind speed.**

Keywords-Surveillance; SSR Mode S; Meteorological Data

I. INTRODUCTION

In recent years, the performance of jet passenger aircraft has been improved by advanced FMS (Flight Management System), IRU (Inertial Reference Unit) and autopilot systems. However, obstacles still exist to realizing the full performance of each aircraft in the current ATC (Air Traffic Control) environment, such as fixed air routes and flight levels, and "radar vectoring" in and around congested terminal airspaces. For these reasons, new concepts for future ATM (Air Traffic Management) systems are being introduced in Europe's SESAR [1] and the United States' NextGen [2] programs to extract maximum benefits from CNS (Communication, Navigation and Surveillance) technologies. CARATS (Collaborative Actions for Renovation of Air Traffic Systems) [3] is a long-term plan to similarly improve Japan's ATM (Air Traffic Management) system, and various research and development projects have been carried out with the aim of achieving greater ATM efficiency.

TBO (Trajectory Based Operations) is one of the key elements in future ATM concepts. TBO will enable jet passenger aircraft to fly along optimal trajectories that maximize their aerodynamic performance. Eventually, it will provide for enhanced time-based air traffic management. The effectiveness of the optimal trajectory and TBO-based ATM rely on the accuracy of meteorological data, so quantitative evaluation of meteorological data is necessary to assess this accuracy. The authors have evaluated NWP data released by the JMA using weather data recorded by jet passenger aircraft, and have studied the accuracy of the JMA-NWP data. The RMSEs of the JMA-NWP data were found to be approximately 3 [m/s] for zonal and meridional wind speed s . [4]

SSR Mode S was developed to reduce radio frequency congestion and enables more aircraft to be handled by radar compared to SSR Mode A/C. In addition, the EHS capability of SSR Mode S downlinks DAPs data which can provide air traffic controllers with detailed information on aircraft within radar coverage. In Japan, many SSR Mode A/C facilities have been replaced with Mode S. However, DAPs data are not yet used positively by ATM systems because only a limited number of aircraft currently have the EHS capability. Considering several recent publications [5] which have used DAPs data in comparative evaluations with NWP models and AMDAR (Aircraft Meteorological Data Relay) and radiosonde observations, we conclude that DAPs is a valuable source of wind speed data.

In this research, JMA-NWP data were statistically evaluated using SSR Mode S DAPs data and the estimation errors of static temperature and wind speed were analyzed. This research aims to contribute towards future ATM systems that can maximize the overall performance of aircraft.

This structure of this paper is as follows. We first describe SSR surveillance data and the estimation methods of static temperature and wind speed. Then, we describe the NWP models released by JMA [6] and evaluate them using RMSE. Finally, we evaluate the effects of the minimum resolution of the DAPs data on estimation errors.

II. SSR SURVEILLANCE DATA

A. Fundamental Parameters of SSR Surveillance Data

SSR Mode S Surveillance Data were acquired by a ground station operated by ENRI (Electronic Navigation Research

Institute) for experimental purposes. Figure 1 shows a photograph of ENRI's SSR ground station and TABLE I lists its main characteristics.

TABLE I. ENRI SSR MAIN CHARACTERISTICS

Item	Property
Radar Site Name	Chofu SSR Mode S Test Ground Station
Position	ENRI (Tokyo, Japan)
Rotation	10 [sec]
Radar Coverage	250 [NM]

Figure 1. ENRI's SSR mode S Experimental Ground Station.

The ground station receives both Mode A/C and Mode S data. As listed in TABLE II, the data consist of Mode A/C basic radar parameters and Mode S additional flight parameters called DAPs including ground speed and true air speed. TABLE II also shows each parameter's minimum resolution. The type of each aircraft can be identified from the aircraft identification number.

TABLE II. SSR MODE S PARAMETERS AND MINIMUM RESOLUTION [7]

Parameter	Minimum Resolution	Data
Time	----	SSR Observation Parameters
Radar Site Flag	----	
Latitude	----	
Longitude	----	
Aircraft Identification Number	----	
Pressure Altitude	25 [ft]	
Ground Speed	2 [kt]	SSR Mode S Downlink Aircraft Parameters (DAPs)
True Air Speed	2 [kt]	
True Track Angle	90/512 [deg]	
Magnetic Heading	90/512 [deg]	
Indicated Air Speed	1 [kt]	
Mach Number	0.004	
Barometric Pressure Setting	0.1 [mb]	
Roll Angle	45/256 [deg]	

Figure 2 shows the position and coverage of the SSR ground station and flight trajectories from a sample of analyzed Mode S data. The experimental ground station is located at about 20 km northeast of Tokyo International Airport (RJTT).

B. Estimation of Meteorological Data

Although SSR Mode S parameters optionally include meteorological routine air report data such as wind speed, wind direction, static temperature, static pressure and humidity, most aircraft do not transmit those parameters. We therefore estimated air temperature and two-dimensional wind speeds, which are necessary meteorological data for ATM, from the DAPs parameters listed in TABLE II as described below.
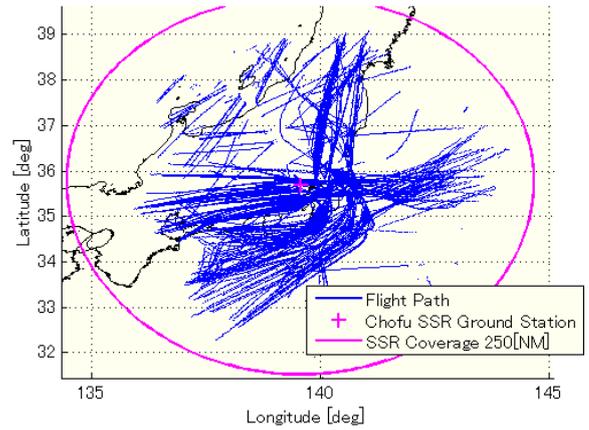

Figure 2. Flight Paths of Analyzed SSR Mode S data.

1) Static temperature

Static temperature T is the function of true air speed V_{TAS} and Mach number M, and is given by (1) below

$$T = \frac{1}{\gamma R}\left(\frac{V_{TAS}}{M}\right)^2 \tag{1}$$

where $\gamma = 1.4$ and $R = 287.05$ [J/(kg·K)].

2) Zonal and meridional wind speed

Zonal wind speed W_{EW} and meridional wind speed W_{NS} are estimated from ground speed V_{GS}, true air speed V_{TAS}, true track angle Ψ_{TRUK} and true heading angle $\Psi_{HDG,TRUE}$ ((2) and (3)):

$$W_{EW} = V_{GS} \sin \Psi_{TRUK} - V_{TAS} \sin \Psi_{HDG,TRUE} \tag{2}$$
$$W_{NS} = V_{GS} \cos \Psi_{TRUK} - V_{TAS} \cos \Psi_{HDG,TRUE} \tag{3}$$

We obtained the true heading angle from magnetic heading angle and magnetic declination, D2010:

$$\Psi_{HDG,TRUE} = \Psi_{HDG,MAG} - D2010 \tag{4}$$

D2010 is the magnetic declination approximation released by the Japan Geographical Survey Institute. The approximation is given by the following quadratic equation (5):

$$D2010 = 7°40.585′ + 19.003′\Delta\phi - 6.265′\Delta\theta + 0.009′\Delta\phi^2 + 0.024′\Delta\phi\Delta\theta - 0.0591′\Delta\theta^2 \tag{5}$$

where $\Delta\phi = \phi - 37°N$ and $\Delta\theta = \theta - 138°E$.

III. JMA NUMERICAL WEATHER PREDICTION GPV DATA

JMA has been developing NWP systems since 1959 and provides a variety of NWP products on national and international regions. In this research, two NWP models are evaluated using DAPs.

GSM (Global Spectral Model) is an NWP model for short- and medium-range forecasts covering the entire globe. It was

developed to express and forecast resolvable motions and the state of the atmosphere with primitive equations. JMA releases global forecasts as GSM (Global) data with a 60 km horizontal resolution and forecasts for Japan and its surrounding local areas as GSM (Japan region) data with a 20 km horizontal resolution. MSM (Meso-Scale Model) is an NWP model for very short-range forecasts covering Japan and its surrounding local areas which was developed to provide information for weather-related disaster prevention and aviation safety. It uses a non-hydrostatic equation for the vertical equation of motion and GSM as its boundary values. TABLE III lists the fundamental parameters of the JMA-NWP models.

NWP models predict the future state of the weather as follows. First, guess fields are generated from the previous model run and observation data obtained from radiosondes, sounding rockets, radar, satellites, and aircraft. Adjustments and model initialization are then applied to generate the starting point of the next numerical simulation run. NWP itself consists of dynamical equations and provides actual status and predicted values.

Mode S data samples obtained at arbitrary horizontal locations were linearly interpolated in longitude and latitude. For vertical interpolation, we obtained static pressure p from recorded QNE pressure altitude H. Within the troposphere ($H < 11000[m]$), static pressure p is obtained by (6):

$$p = p_0 \left(\frac{bH}{T_0} + 1 \right)^{-\frac{g}{bR}} \qquad (6)$$

where $p_0 = 1013.250[hPa]$, $b = -0.0065[K/m]$, $T_0 = 288.15[K]$, $g = 9.80665[m/s^2]$.

In the stratosphere ($H \geq 11000[m]$), static pressure p is obtained by (7):

$$p = p_1 \exp\left[-\frac{g}{RT_1}(H - 11000) \right] \qquad (7)$$

where $p_1 = 226.55[hPa]$, $T_1 = 216.65[K]$.

Linear interpolation was also used between the arbitrary recorded times of each data point. In order to make an analysis of the prediction time and forecast accuracy, five predicted values were evaluated in the interval from 0 to 24 hours predicted time. Figures 3 and 4 illustrate recorded times of SSR data, evaluated values of GSM and MSM, and initial values.

For example, when evaluating GSM predicted values generated for 12 hours beforehand with SSR data (09-10UTC), 12-hour and 18-hour prediction values forecasted at 00UTC are interpolated and evaluated. On the other hand, when evaluating MSM predicted values generated for 12 hours beforehand with SSR data (09-10UTC), 12-hour and 15-hour prediction values forecasted at 21UTC are interpolated and evaluated because the MSM predicted values are generated every 3 hours, while GSM predicted values are generated every 6 hours.
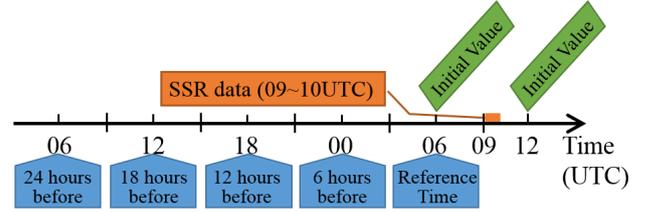

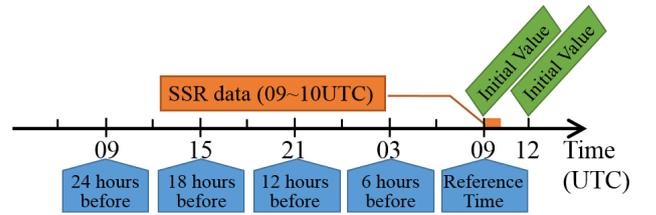Figure 3.   Definition of Evaluated Forecast Data (GSM).

Figure 4.   Definition of Evaluated Forecast Data (MSM).

ME (Mean Error) and RMSE are used to evaluate the accuracy of JMA-NWP data statistically. ME is defined in (8) and RMSE is defined in (9):

$$ME = \frac{1}{N} \sum_{i=1}^{N} (X_{DAPs} - X_{GPV}) \qquad (8)$$

$$RMSE = \sqrt{\frac{1}{N} \sum_{i=1}^{N} (X_{DAPs} - X_{GPV})^2} \qquad (9)$$

where N is the number of data points, X_{DAPs} are evaluation values estimated by DAPs, and X_{GPV} are corresponding values of the JMA-NWP data.

TABLE III.   SPECIFICATIONS OF JMA-NWP MODELS [8]

Item	GSM (Global Spectral Model)		MSM (Meso-Scale Model)
	Global	*Japan region*	
Purpose	Short- and medium-range forecast		Very-short- range forecast
Initial time value	00, 06, 12, 18UTC		00, 03, 06, 09, 12, 15, 18, 21UTC
Forecast domain	Globe	Latitude: 20-50 deg Longitude: 120-150 deg	Latitude: 22.4-47.6 deg Longitude: 120-150 deg
Resolution or number of grids	0.1875 deg (TL959)		5km 721 x 577
Barometric pressure levels/ Top	60 levels/ 0.1 hPa		50 levels/ 21,800 m
Forecast hours (Initial time)	84 hours (00, 06, 18UTC) 264 hours (12 UTC)		39 hours (00, 03, 06, 09, 12, 15, 18, 21UTC)
Simulation model	Hydrostatic model		Non-hydrostatic model
Data assimilation	Global Analysis (GA)		Meso-Scale Analysis (MA)
Assimilation method	4D-Var analysis		
Physical variables	Geopotential altitude, temperature, vertical flow, relative humidity, wind velocity		

IV.   EVALUATION OF JMA-NWP DATA

A. Analysis Example

First, we present an analysis example. The case shown in Figure 5 is a Boeing 777-200 aircraft departing from Narita International Airport (RJAA) in Dec. 2013. Figures 6 to 8 illustrate the time histories of roll angle, pressure altitude and velocity. Figures 9 and 10 show time histories of static temperature and wind speed from DAPs data and corresponding actual status values from JMA-NWP data. GSM (Japan region) data are not shown in these figures because they are almost identical to the GSM (Global) values.
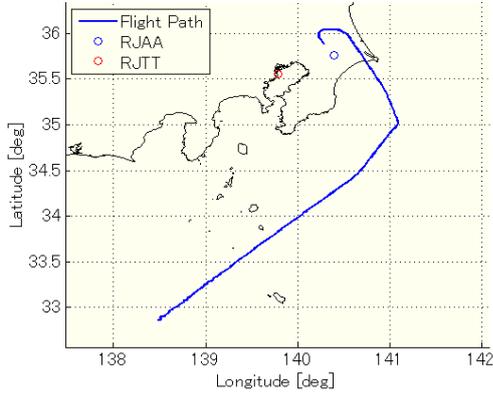
Figure 5.   Flight Path of Model Case.
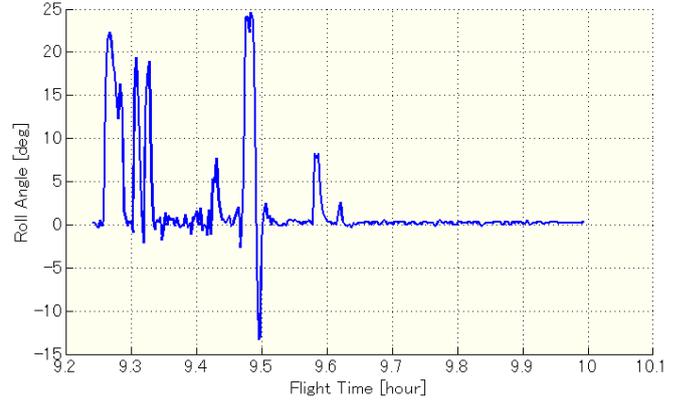
Figure 6.   Roll angle (Positive: Right Wing Down).
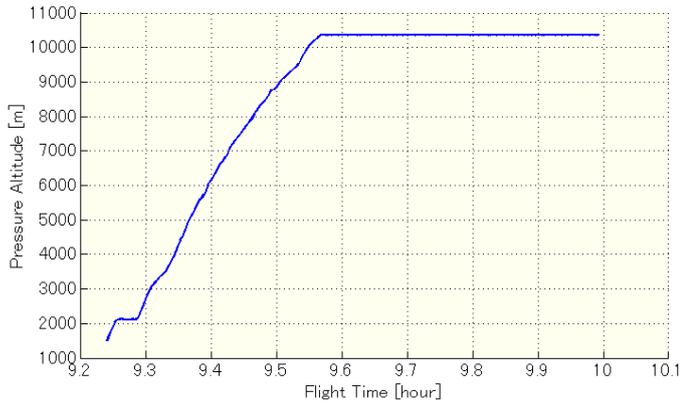
Figure 7.   Pressure Altitude.
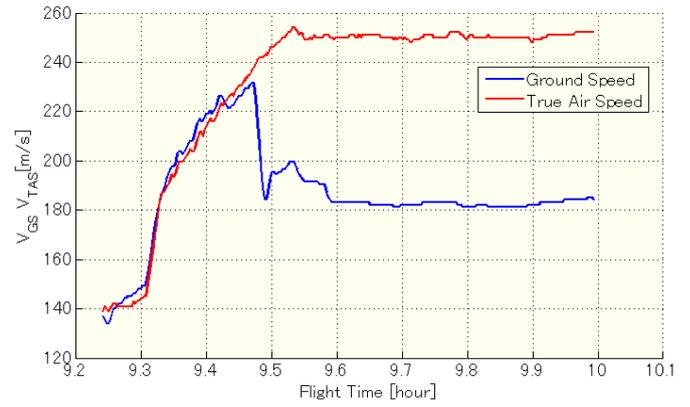
Figure 8.   Ground Speed and True Air Speed.
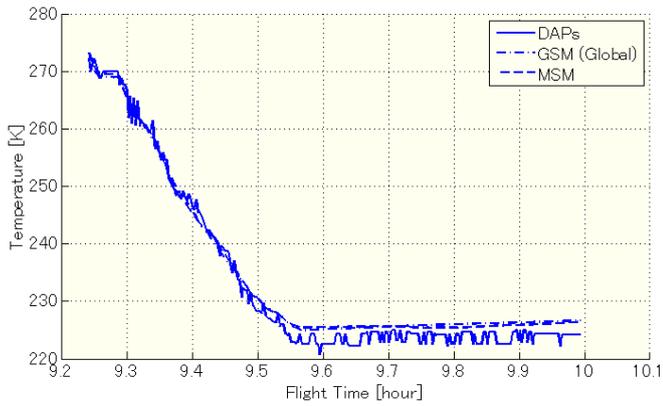
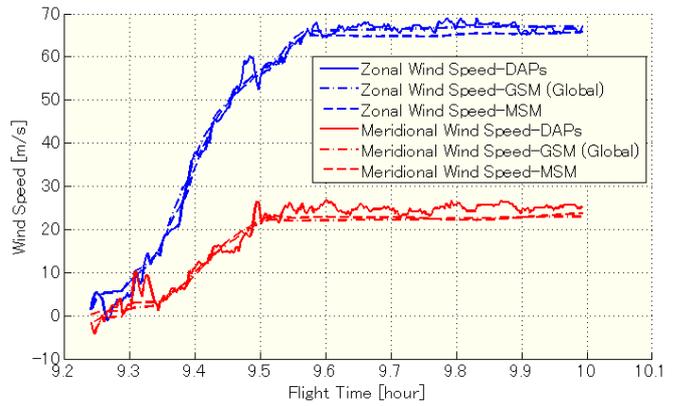Figure 9.   Time History of Static Temperature.

Figure 10. Time History of Zonal and Meridional Wind Speed.

Figures 5 and 6 show that the aircraft made a right turn after takeoff and then flew in a southwesterly direction. Figures 7 and 8 show that the aircraft climbed to FL340. The time history of static temperature in Figure 9 shows that the DAPs data and the JMA-NWP (GSM and MSM) data are almost the same in all flight phases. The RMSE of GSM (Global) was 1.83 [K]. Figure 10 shows that the JMA-NWP wind data accord with the DAPs data, the RMSE of GSM (Global) being 2.13 [m/s] for zonal wind speed. However, Figures 6 and 10 show that there is a considerable difference between DAPs and the NWPs during the turn maneuvers.

B. 12 Month Analysis

A total of twelve hours of SSR mode S DAPs data for different seasons were statistically analyzed. The data consisted of twelve sets of the same one-hour periods from 09Hrs. UTC taken from each month of 2013. The time period corresponds to one of the Tokyo metropolitan area's air traffic peaks.

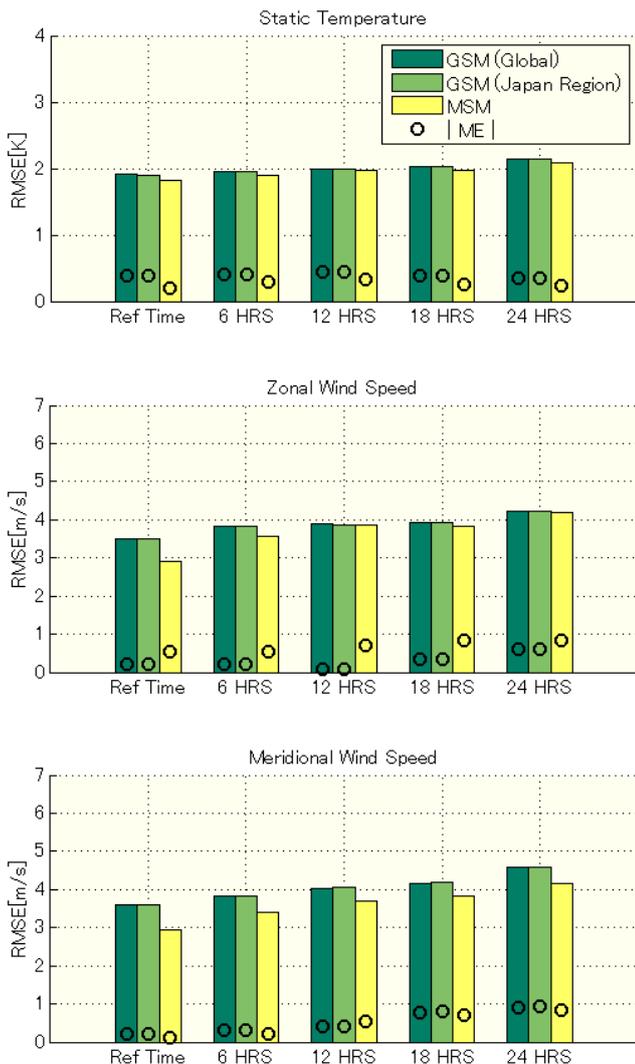Figure 13 illustrates the result of the absolute value of ME and the RMSE of the JMA-NWP data.

'Ref Time' means that the evaluation results of the JMA-NWP data were released at reference time. The metrological data are interpolated between the initial value and 6 hours prediction. Similarly, '6 HRS', '12 HRS', '18 HRS', '24 HRS' mean that the evaluation results of the JMA-NWP data were released at the corresponding time as explained by Figures 3 and 4.

Although the grid point resolution of GSM (Global) is coarser than that of GSM (Japan region), the prediction accuracies of GSM (Global) and GSM (Japan region) are about the same. This is because GSM (Global) and GSM (Japan region) are essentially derived from the same NWP model.

Figure 11 shows that the RMSEs of MSM are rather smaller than those of GSM at the reference time; approximately 1.82 [K] for static temperature and about 3.0 [m/s] for wind speed. The prediction accuracy gradually deteriorates with increasing prediction time for each parameter. The RMSE is increased by 0.3 [K] for 24 hours, while the prediction accuracy of zonal and meridional wind speeds deteriorates along with the prediction time. The RMSE increases by 1.0 [m/s] for 24 hours. In particular, the RMSE of MSM zonal wind speed is smaller than that of GSM by 0.5 [m/s]; however the RMSE of MSM and GSM are almost the same.

C. High/ Low Altitude Analysis

Figures 12 to 15 illustrate the prediction accuracies at low altitude (H < 10000[ft]) and high altitude (H ≥ 29000[ft]).

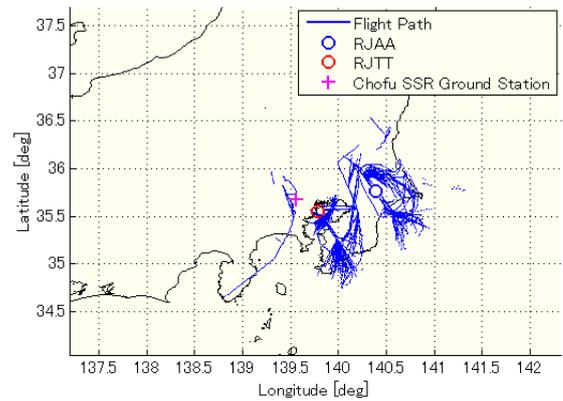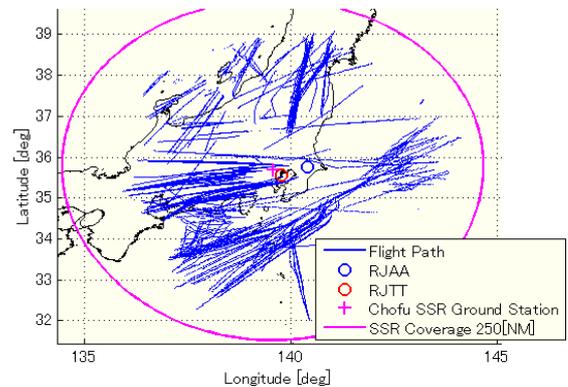Figure 12. SSR Mode S data (H < 10000[ft]).

Figure 13. SSR Mode S data (H ≥ 29000[ft]).
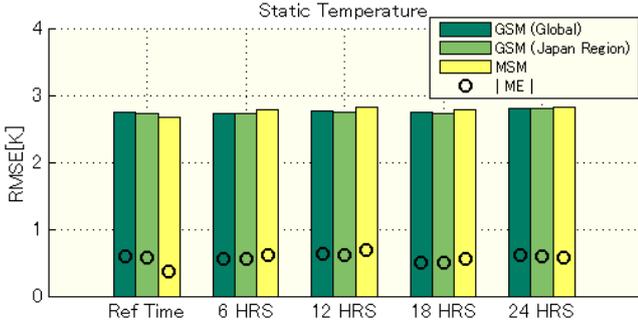

Figure 11. RMSE of the JMA-WNP data (Meridional Wind Speed).

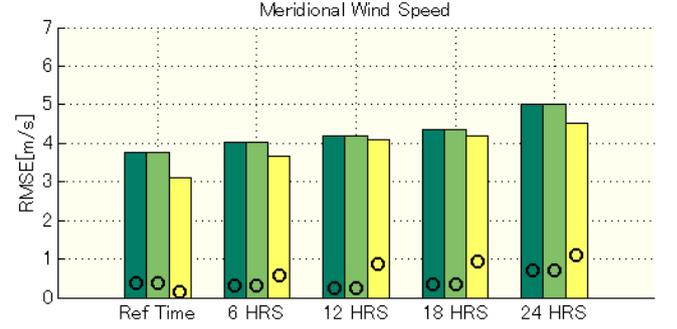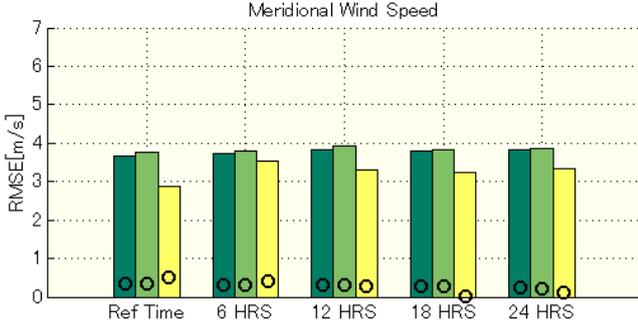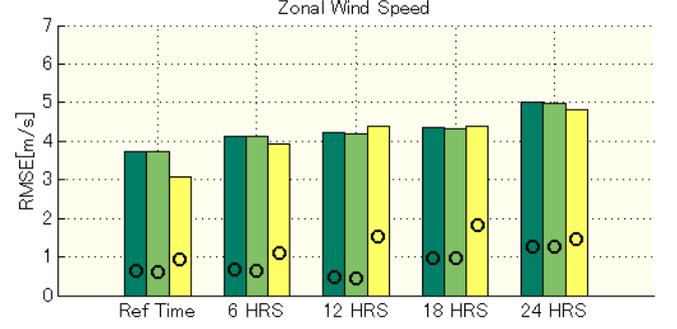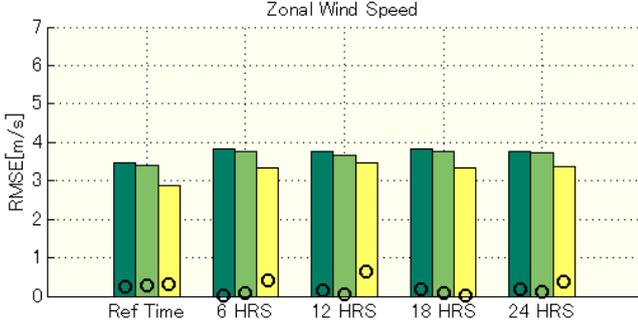Figure 14. RMSE of the JMA-WNP data. ($H < 10000[ft]$)
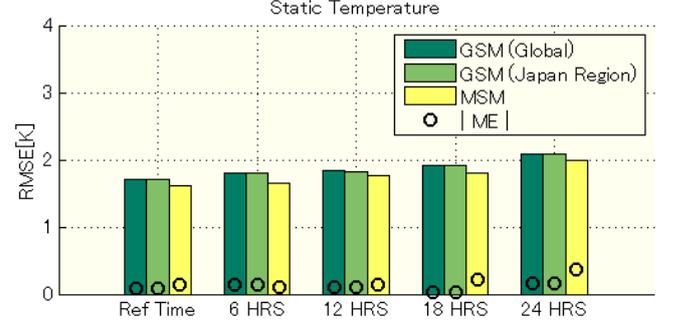
Figure 15. RMSE of the JMA-WNP data. ($H \geq 29000[ft]$)

Figures 12 and 13 show the positions of DAPs data samples lower than 10000 [ft] and higher than 29000 [ft], respectively. Almost all the aircraft at low altitude are departing from or approaching to RJAA and RJTT.

The results in Figures 14 and 15 show that the RMSE of static temperature increases by 1.0 [K] at low altitude for all prediction values. This difference is due to error caused by the minimum resolution of DAPs data, discussed in section V. RMSE at high altitude increases by 0.5 [K] along with the prediction time, while RMSE at low altitude is almost constant. Figure 14 shows that the RMSE at low altitude is about 3-4 [m/s], almost constant with changing prediction time. On the other hand, the RMSE at high altitude shown in Figure 15 increases by 1.0 [m/s] along with the prediction time.

We suppose that the prediction accuracy for the upper atmosphere is lower than for the lower atmosphere due to relatively lower density of upper atmospheric observations.

V. ESTIMATION ERROR

In the previous section, the prediction accuracy of the JMA-NWP data was evaluated assuming that the values derived from DAPs data are the true values. However, due to the low resolution of the DAPs downlink parameters (see TABLE I), the analyzed static temperature and wind speed are subject to estimation errors. In this section, the estimation errors due to the minimum resolution of DAPs parameters are analyzed.

A. Staic Temperature

Static temperature is the function of true air speed V_{TAS} and Mach number M. The subscript DAPs denotes DAPs downlink parameter values and quantities derived directly those values. Static temperature T_{DAPs} is obtained by (10)

$$T_{DAPs} = \frac{1}{\gamma R} \left(\frac{V_{TAS\_DAPs}}{M_{DAPs}} \right)^2 \tag{10}$$
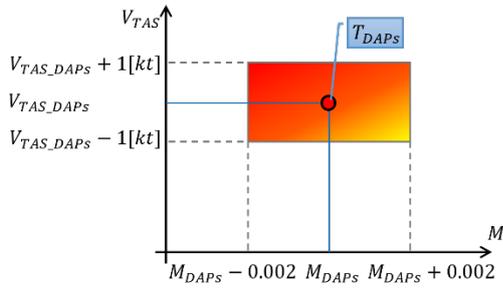
Figure 16. Estimation Error of Static Temperature.

TABLE II lists the minimum resolutions of each DAPs parameter. The true values of true air speed and Mach number exist within the ranges shown in (11) and (12):

$$V_{TAS\_DAPs} - 1[kt] < V_{TAS} \leq V_{TAS\_DAPs} + 1[kt] \quad (11)$$
$$M_{DAPs} - 0.002 < M \leq M_{DAPs} + 0.002 \quad (12)$$

It can be assumed that the distributions of the true values of true air speed and Mach number are uniform. Then, the probability density distribution function p_T becomes (13) given minimum resolutions of Mach number ΔM and true air speed ΔV_{TAS}.

$$p_T(M, V_{TAS}) = \frac{1}{\Delta M \cdot \Delta V_{TAS}} \quad (13)$$

The estimation error (RMSE) is defined as (14)

$$RMSE_T = \left\{ \int_{M_{DAPs}-0.002}^{M_{DAPs}+0.002} \int_{V_{TAS_{DAPs}}-1[kt]}^{V_{TAS_{DAPs}}+1[kt]} p_T \left[\frac{1}{\gamma R} \left(\frac{V_{TAS}}{M} \right)^2 - T_{DAPs} \right]^2 dV_{TAS} dM \right\}^{1/2} \quad (14)$$

B. Zonal and Meridional Wind Speed

As with the error estimation of static temperature, zonal and meridional wind speed are obtained using (15) and (16).

$$W_{EW\_DAPs} = V_{GS\_DAPs} \sin \Psi_{TRUK\_DAPs} - V_{TAS\_DAPs} \sin \Psi_{HDG\_DAPs} \quad (15)$$

$$W_{NS\_DAPs} = V_{GS\_DAPs} \cos \Psi_{TRUK\_DAPs} - V_{TAS\_DAPs} \cos \Psi_{HDG\_DAPs} \quad (16)$$

The minimum resolutions of these parameters are listed in TABLE II. The true values of each parameter are within the ranges shown in (17) to (20).

$$V_{GS\_DAPs} - 1[kt] < V_{GS} \leq V_{GS\_DAPs} + 1[kt] \quad (17)$$

$$V_{TAS\_DAPs} - 1[kt] < V_{TAS} \leq V_{TAS\_DAPs} + 1[kt] \quad (18)$$

$$\Psi_{HDG\_DAPs} - 45/512 \,[deg] < \Psi_{HDG} \leq \Psi_{HDG\_DAPs} + 45/512 \,[deg] \quad (19)$$

$$\Psi_{TRUK\_DAPs} - 45/512 \,[deg] < \Psi_{TRUK} \leq \Psi_{TRUK\_DAPs} + 45/512 \,[deg] \quad (20)$$

A uniform distribution p_W is used to estimate RMSE. p_W is defined by (21) where delta defines the minimum resolution of each parameter.

$$p_W(V_{GS}, \Psi_{TRUK}, V_{TAS}, \Psi_{HDG})$$
$$= \frac{1}{\Delta V_{GS} \cdot \Delta \Psi_{TRUK} \cdot \Delta V_{TAS} \cdot \Delta \Psi_{HDG}} \quad (21)$$

The estimation error (RMSE) is obtained by (22) and (23).

$$RMSE_{W_{EW}} = \left\{ \int^{(4)} p_W [(V_{GS} \sin \Psi_{TRUK} - V_{TAS} \sin \Psi_{HDG}) - W_{EW\_DAPs}]^2 dV_{GS} dV_{TAS} d\Psi_{HDG} d\Psi_{TRUK} \right\}^{1/2} \quad (22)$$

$$RMSE_{W_{NS}} = \left\{ \int^{(4)} p_W [(V_{GS} \cos \Psi_{TRUK} - V_{TAS} \cos \Psi_{HDG}) - W_{NS\_DAPs}]^2 dV_{GS} dV_{TAS} d\Psi_{HDG} d\Psi_{TRUK} \right\}^{1/2} \quad (23)$$

C. Results of Estimation Error

Figure 17 shows the relationship between Mach number and pressure altitude and Figure 18 show the relationship between estimation error of wind speed and true track angle.
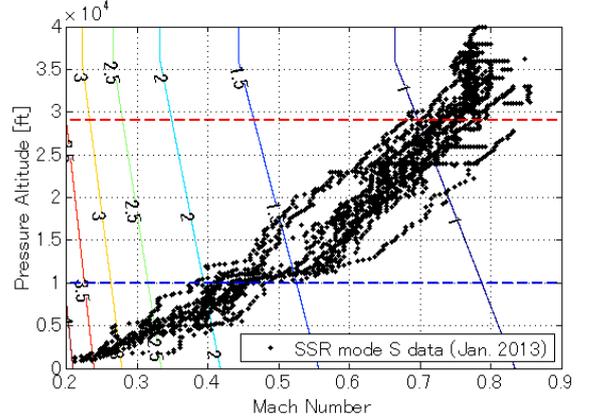

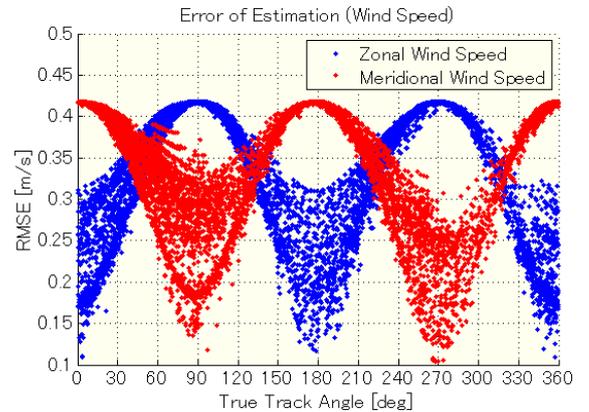Figure 17. Estimation Error on Static Temperature (RMSE).

Figure 18. Estimation Error on Wind Speed (RMSE).

Figure 17 shows a contour map of RMSE estimation error and a plot of DAPs data (Jan. 2013). At low altitudes (lower than 10000 [ft]) the estimation error is more than 1.5 [K]. On

the other hand, at high altitudes (higher than 29000 [ft]) the estimation error is less than 1.0 [K]. In this analysis, static temperature estimated from DAPs values includes a relatively large estimation error, particularly when pressure altitude and Mach number are low.

Figure 18 clearly indicates that estimation errors of zonal and meridional wind speed are related to true track angle.
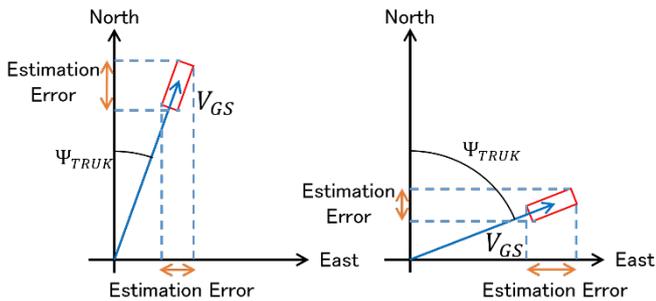

Figure 19. Minumum Resolution of Velocity Vector and Estimation Error.

Figure 19 illustrates a velocity vector (e.g. ground speed vector) and its error (red square). The minimum resolution of ground speed (2 [kt]) is relatively larger than that of true track angle (0.176 [deg]). Therefore, in case of a true track angle that is directly North or South, the estimation error of meridional wind speed becomes larger than that of zonal wind, while for a true track angle that points directly East or West the estimation error of zonal wind speed becomes larger than that of meridional wind.

TABLE IV lists the mean values of RMSE (estimation error) on each data point.

TABLE IV.   ESTIMATION ERROR DUE TO MINIMUM RESOLUTION

	Static Temperature	Zonal Wind Speed	Meridional Wind Speed
Estimation Error (RMSE)	1.51 [K]	0.33 [m/s]	0.33 [m/s]

Compared with the RMSE of the JMA-NWP data, the estimation error of static temperature is large while estimation errors of zonal and meridional wind speed are relatively small. This clearly illustrates that static temperature includes an estimation error of about 1.5 [K].

VI.   CONCLUSIONS

DAPs of SSR mode S were used to statistically evaluate the accuracy of JMA-NWP models. The analysis of different seasons' twelve hours data reveals,

- The RMSE of JMA-NWP data compared with DAPs at reference time, zero prediction time, is about 2.0 [K]

for static temperature, and about 3.0 [m/s] for wind speed.

- MSM gives slightly better performance than GSM statistically, but the difference is not so pronounced.

- Accuracy slightly decreases with increasing prediction time, where RMSE increases by 0.3 [K] and 1.0 [m/s] at 24 hours prediction.

- NWP for lower altitudes are slightly more accurate than for upper altitudes. The difference increases with prediction time.

The estimation errors due to DAPs parameter resolution were evaluated analytically.

- The estimation errors due to the resolution of downlinked values is about 1.5 [K] and 0.33 [m/s] in average.

- Estimation errors due to DAPs resolution are large for static temperature, accounting for about half of the total RMSE. On the other hand, in case of wind speed, it comprises only 10% of the total RMSE.

The results and method described in this paper are useful for quality assurance of the NWP model for ATM systems. Accurate wind forecasting is a critical element of Trajectory-Based Operations proposed for future ATM. What level of accuracy is necessary for ATM, and what kind of improvements in wind forecasting are made possible by using DAPs, are problems to be investigated.

REFERENCES

[1]   SESAR Joint Undertaking, European ATM Master Plan 2nd Edition, October, 2012.

[2]   Federal Aviation Administration, NextGen Implementation Plan, June, 2013.

[3]   Ministry of Lnad, Infrastructure and Transport, "Collaborative Actions for Renovation of Air Traffic Systems," 2010. [Online]. Available: http://www.mlit.go.jp/common/000128185.pdf.

[4]   H. Totoki, T. Kozuka, Y. Miyazawa , K. Funabiki, "Comparison of JMA Numerical Prediction GPV Meteorological Data and Airliner Flight Data (in Japanese)," Aerospace Technology Japan, The Japan Society for Aeronautical and Space Sciences, 12, 2013.

[5]   S. d. Haan, "Quality Asessment of High Resolution Wind and Temperature Observation from ModeS," KNMI publication: WR-2010-03, 2010.

[6]   Japan Meteorological Agency, "Numerical Weather Prediction Activities," [Online]. Available: http://www.jma.go.jp/jma/en/Activities/nwp.html.

[7]   ICAO, Technical Provisions for Mode S Services and Extended Squitter, Doc 9871.

[8]   Japan Meteorological Business Support Center Online Data Service, [Online]. Available: http://www.jmbsc.or.jp/hp/online/f-online0.html.